JOURNAL OF COMPUTATIONAL PHYSICS 80, 331–343 (1989)

Interpolation on a Triangulated 3D Surface

THOM F. OOSTENDORP, ADRIAAN VAN OOSTEROM, AND GEERTJAN HUISKAMP

Laboratory of Medical Physics and Biophysics, University of Nijmegen, the Netherlands

Received August 4, 1987; revised January 4, 1988

An interpolation method for scalar functions on a rectangular grid on a planar surface is extended to the interpolation function on a closed three-dimensional triangulated surface of arbitrary shape. Two variants are considered. The first one constrains the Laplacian of the function to be zero at points where the function values are unknown. The second one minimizes the Laplacian at all points of the surface considered. Some illustrative examples of both variants are given in applications to the display of potential distributions on the boundary surface of an electrical volume conductor.

I. INTRODUCTION

A problem often encountered in various fields of research is that of obtaining an acceptable approximation of a scalar function f defined on a closed surface in three-dimensional space, for which the function values are available (for instance, by measurement) at a limited number of points on this surface only. There are numerous methods for interpolating the value of f at any given point on the surface if the function values are known at all nodal points of a mesh of this surface [8]. In this paper we shall discuss the case in which the function values are known for a subset of the nodes only.

One of the methods for solving this problem for a regular, rectangular mesh on a planar surface was presented by Heringa *et al.* [7]. The points at which the value of f is given form a subset of the points of this mesh. The values of f at all other points of the mesh are found by requiring the value of f at these points to be equal to the straight average of the values at the neighbouring points. This procedure constructs a smooth function, the values of which coincide with the true values at the points where f is known.

This method can be extended to a non-regular rectangular mesh. In that case the function value at a point is assigned a weighted average of the values at its direct neighbours. The weighting coefficients depend on the distance between the points. This method can be modelled by a resistance network, where the potential is fixed at some points and the potential at all other points is found by applying Kirchhoff's law. The resistances in this model represent the weighting coefficients.

0021-9991/89 $3.00

581/80/2-6

A similar way to construct a smooth interpolation is to put constraints on the Laplacian Δf of the function, i.e.,

$$\Delta f = \left(\frac{\partial^2}{\partial x^2} + \frac{\partial^2}{\partial y^2}\right) f. \tag{1}$$

The choice of the Laplacian to construct a smooth function is just one of the many that can be made. It has been used in as widely different fields as the solution of integral equations [11] and digital picture processing [13]. As the Laplacian of a function at a point can be estimated in a rectangular mesh as a weighted sum of the value at that point and at its direct neighbours, the method described above can be looked upon as an approximation of the constraint $\Delta f = 0$.

In the case of a function defined on a curved surface in three-dimensional space we have to consider $\Delta_s f$ instead of Δf:

$$\Delta_s f = \left(\frac{\partial^2}{\partial x^2} + \frac{\partial^2}{\partial y^2}\right) f, \tag{2}$$

in which x and y are local surface coordinates.

A rectangular mesh is not suited for representing a surface of arbitrary shape in three dimensions; such a surface is more adequately described by a triangular mesh. So the first extension to the interpolation method is that we shall construct an estimate of $\Delta_s f$ on a triangular mesh. Another extension which we shall present is a method which minimizes $\Delta_s f$ at all points without changing the values at the prescribed points.

II. Estimate of $\Delta_s f$ in a Triangular Mesh

We start by considering the well-known results for the rectangular mesh. Consider p_0 in such a mesh with neighbours $p_1 \cdots p_4$. We will denote f_i the value of f at point p_i. Let (x, y) be the position of p_0. A Taylor expansion in the x coordinate yields

$$f(x+h, y) \simeq f(x, y) + h \left.\frac{\partial f}{\partial x}\right|_{p_0} + \frac{1}{2} h^2 \left.\frac{\partial^2 f}{\partial x^2}\right|_{p_0}, \tag{3}$$

or

$$f_1 \simeq f_0 + h \left.\frac{\partial f}{\partial x}\right|_{p_0} + \frac{1}{2} h^2 \left.\frac{\partial^2 f}{\partial x^2}\right|_{p_0}. \tag{4a}$$

Similarly, for the y coordinate one has

$$f_2 \simeq f_0 + h \left.\frac{\partial f}{\partial y}\right|_{p_0} + \frac{1}{2} h^2 \left.\frac{\partial^2 f}{\partial y^2}\right|_{p_0}. \tag{4b}$$

A similar expression can be found for f_3 and f_4. Addition of these four expressions yields

$$f_1+f_2+f_3+f_4 \simeq 4f_0+h^2\left(\frac{\partial^2}{\partial x^2}+\frac{\partial^2}{\partial y^2}\right)f\,|_{p_0}=4f_0+h^2\,\Delta f_0, \tag{5}$$

thus

$$\Delta f_0 \simeq \frac{1}{h^2}\left(\sum_{i=1}^{4} f_i-4f_0\right),$$

i.e.,

$$\Delta f_0 \simeq \frac{4}{h^2}(\bar{f}-f_0), \tag{6}$$

in which $\bar{f}$ is the average of $f_1 \cdots f_4$. This is the well-known first-order estimate of the Laplacian Δ in a regular rectangular mesh at p_0 [1].

Now consider a regular planar triangular mesh. In this mesh each point has six neighbours instead of four. We can extend the estimation of Eq. (5) to

$$\Delta f_0 \simeq \frac{4}{h^2}(\bar{f}-f_0), \tag{7}$$

in which $\bar{f}$ is now the average of $f_1 \cdots f_6$, i.e., the average of the function value at all neighbouring points. This expression holds true for any n points regularly distributed on a circle having a radius h around the reference point p_0 as can be seen by applying a Taylor expansion to any point p_i with coordinates $x_i = x(p_0)+h\cos(\phi_i)$; $y_i = y(p_0)+h\sin(\phi_i)$, and using the orthonormality properties of points evenly distributed on a circle.

In an irregular planar triangular mesh the number of neighbours and their relative position and distance differ from point to point. Let n be the number of neighbours p_i $(i=1, n)$ of any point p_0, and h_i the distance between p_i and p_0. We now extend Eq. (7) to this situation. When not all neighbours are at the same distance we use a linear approximation of f on the line between p_0 and p_i. Let $\bar{h}$ be the average of $h_1 \cdots h_n$, i.e., the mean distance between p_0 and its neighbours. The linear approximation to f for points $\tilde{p}_i$ at a distance $\bar{h}$ from p_0 on the line from p_0 to p_i then reads

$$\tilde{f}_i \simeq f_0+\frac{\bar{h}}{h_i}(f_i-f_0). \tag{8}$$

Now we have the values at n points at distance $\bar{h}$ from p_0, so we can extend Eq. (7) by replacing h by $\bar{h}$ and $\bar{f}$ by the mean value of the $\tilde{f}_i$'s,

$$\Delta f_0 \simeq \frac{4}{\bar{h}^2}\left(\frac{1}{n}\sum_{i=1}^{n}\tilde{f}_i-f_0\right),$$

$$=\frac{4}{\bar{h}^2}\left(\frac{1}{n}\sum_{i=1}^{n}\left\{f_0+\frac{\bar{h}}{h_i}(f_i-f_0)\right\}-f_0\right),$$

hence

$$\Delta f_0 \simeq \frac{4}{\bar{h}}\left(\frac{1}{n}\sum_{i=1}^{n}\frac{f_i}{h_i} - \overline{\left(\frac{1}{h}\right)} f_0\right). \tag{9}$$

When the points p_i are not distributed at regular angles around p_0, Eq. (9) may not be a very accurate estimation of the Laplacian as such. We have tried an expression that accounts for irregular angles. Although this expression gives a better approximation of the Laplacian on a planar surface, it does not give better results when used as a constraint in the interpolation procedure (closed surface in 3-dimensional space). As this expression is more complicated, we will use the approximation given by Eq. (9) as a constraint in the interpolation procedure to be described. We will use this estimate of Δf on a planar triangular mesh as an estimate of $\Delta_s f$ on a closed triangulated surface in three-dimensional space.

III. Interpolation Procedure

Consider a triangular mesh on a three-dimensional surface (Fig. 1). Let N be the number of points in this mesh. The function values f_i at points p_i, $i = 1, K$ are to be found through interpolation; those at points p_i, $i = K+1, N$ are assumed to be known. The Laplacian Δ_s can be expressed as a matrix L, defined by

$$l_{ii} = -\frac{4}{\bar{h}_i}\overline{\left(\frac{1}{h_i}\right)},$$

$$l_{ij} = \frac{4}{\bar{h}_i}\frac{1}{n_i}\frac{1}{h_{ij}} \qquad \text{for} \quad i \neq j,\ p_j \text{ direct neighbour of } p_i,$$

$$l_{ij} = 0 \qquad \text{for} \quad i \neq j,\ p_j \text{ no direct neighbour of } p_i,$$

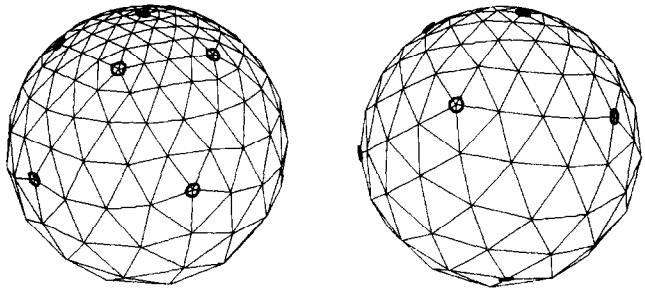

a b

FIG. 1. Triangular mesh of a sphere. The points which are used as "electrode points" are indicated by bold circles. Fiogure 1a is an anterior view, from slightly above, and Fig. 1b is a posterior view.

with

h_{ij}, distance between p_i and p_j;

n_i, number of neighbours of p_i;

$\bar{h}_i$, average of h_{ij} over the neighbours of i;

$\overline{(1/h_i)}$, average of $1/h_{ij}$ over the neighbours of i.

Now we have for the Laplacian of f at point i,

$$(\Delta_s f)_i \simeq \sum_{j=1}^{N} l_{ij} f_j,$$

or,

$$\mathbf{v} = L\mathbf{f},$$

in which $\mathbf{v}$ is the vector containing elements $v_i = (\Delta_s f)_i$.

The vector $\mathbf{f}$ can be split into two parts $\mathbf{f}_1$ and $\mathbf{f}_2$, $\mathbf{f}_1$ related to points 1 to K, and $\mathbf{f}_2$ related to the remaining points. The vector $\mathbf{f}_1$ contains the unknown values, and $\mathbf{f}_2$ contains the values specified. In a similar way we can partition L into four parts

$$L = \begin{pmatrix} L_{11} & L_{12} \\ L_{21} & L_{22} \end{pmatrix},$$

and $\mathbf{v}$ into $\mathbf{v}_1$ and $\mathbf{v}_2$.

Method A: $\Delta_s f = 0$ at Points Where f Is not Given

The condition $(\Delta_s f)_i = 0$ for $i = 1$ to K (i.e., at all points where f is not given; equivalent to using the analogon of a resistance network) leads to solving the equation

$$\mathbf{v}_1 = (L_{11} L_{12}) \begin{pmatrix} \mathbf{f}_1 \\ \mathbf{f}_2 \end{pmatrix} = L_{11}\mathbf{f}_1 + L_{12}\mathbf{f}_2 = \mathbf{0},$$

or

$$L_{11}\mathbf{f}_1 = -L_{12}\mathbf{f}_2.$$

This is a set of K linear equations in K variables. This set is not singular as can immediately be appreciated by considering the implied physical model (resistance network). Consequently this set can easily be solved, e.g., by Gaussian elimination with partial pivoting [5, Chap 3].

Method B: Minimize $\Delta_s f$ at All Points

In Method A the interpolated function values were found by requiring $\Delta_s f$ to be zero at the points where f is not given. As a result the function will be smooth at these points, but may not be smooth at all at the points where f is given. Intuitively, this non-uniform application of the constraint to the two sets of points considered is not immediately obvious. We shall now demonstrate that the constraint may be imposed uniformly, while still retaining the values at the points where f is given. In that case we still have K variables, but we have N equations: one equation for $\Delta_s f$ at each point. Since we now have more equations than variables there is, in general, no solution to the demand $\Delta_s \mathbf{f} = \mathbf{0}$. Instead, we relax the demand on $\Delta_s \mathbf{f}$, and require it to be minimal in a least squares sense. Hence we want to minimize the Euclidean norm $|\mathbf{v}|$ of $\mathbf{v}$,

$$|\mathbf{v}| = |L\mathbf{f}| = \left| \begin{pmatrix} L_{11} & L_{12} \\ L_{21} & L_{22} \end{pmatrix} \begin{pmatrix} \mathbf{f}_1 \\ \mathbf{f}_2 \end{pmatrix} \right|$$

$$= \left| \begin{pmatrix} L_{11} \\ L_{21} \end{pmatrix} \mathbf{f}_1 + \begin{pmatrix} L_{12} \\ L_{22} \end{pmatrix} \mathbf{f}_2 \right|.$$

This is equivalent to finding the least squares solution to

$$\begin{pmatrix} L_{11} \\ L_{21} \end{pmatrix} \mathbf{f}_1 = -\begin{pmatrix} L_{12} \\ L_{22} \end{pmatrix} \mathbf{f}_2, \tag{10}$$

which is a system of N equations in K variables. The well-known least squares solution to this system of equations is

$$\mathbf{f}_1 = -\left(\begin{pmatrix} L_{11} \\ L_{21} \end{pmatrix}^t \begin{pmatrix} L_{11} \\ L_{21} \end{pmatrix} \right)^{-1} \begin{pmatrix} L_{11} \\ L_{21} \end{pmatrix}^t \begin{pmatrix} L_{12} \\ L_{22} \end{pmatrix} \mathbf{f}_2. \tag{11}$$

The solution to Eq. (10) may be computed directly from Eq. (11), using some appropriate numerical routine for the matrix inversion of the non-singular matrix involved. In the results to be presented Eq. (10) was solved directly by using the routine HFTI [9], which provides the general least squares solution. For large systems it may be advisable to use the sparseness of the system [4]. When considering the use of methods for solving sparse systems the complication due to the fact that the bandwidth is, in general, not uniform has to be taken into account. This is the case when the vertex points are surrounded by a non-uniform number of neighbours.

IV. Results

This section demonstrates the application of the methods described above in a number of examples.

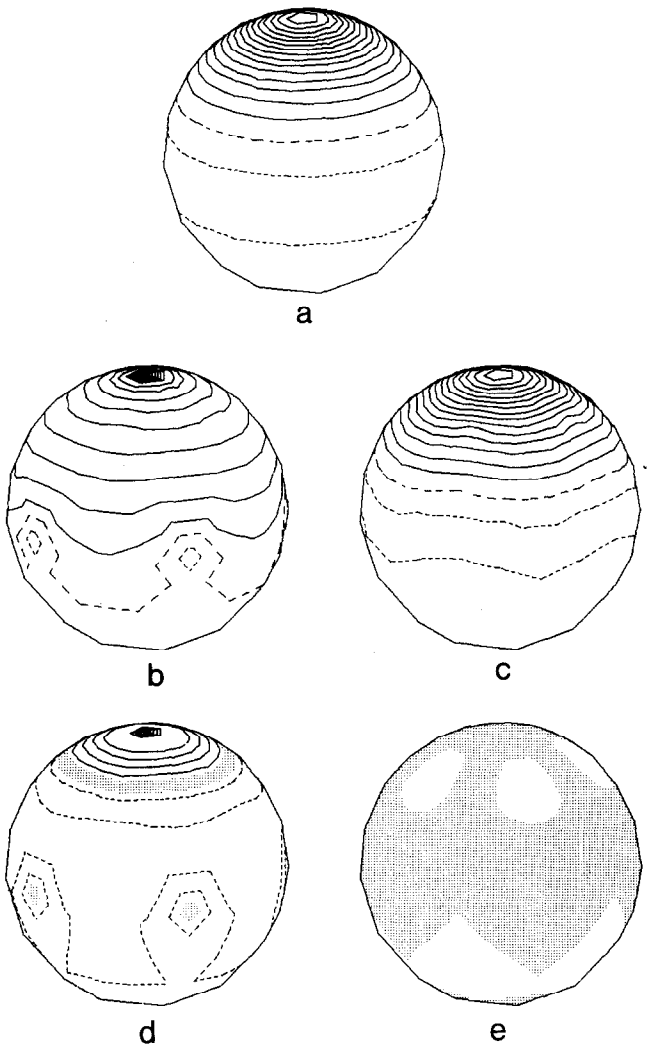

FIG. 2. Plots of isopotential lines on the mesh of Fig. 1 (anterior view). The stepsize between the isopotential lines is the same in all plots. Negative lines are dashed. The zero line is dashed in larger segments. In the difference plots (Figs. 2d and e) the area within half a stepsize around zero is shaded: (a) potential distribution on the sphere generated by a current dipole inside the sphere as computed analytically; (b) potential distribution estimated from the potentials at the electrode points (see Fig. 1) as computed by Method A; (c) potential distribution estimated from the potentials at the electrode points (see Fig. 1) as computed by Method B; (d) difference between the result of Method A (Fig. 2b) and the actual potential distribution (Fig. 2a); (e) difference between the result of Method B (Fig. 2c) and the actual potential distribution (Fig. 2a).

(a) Consider a sphere of radius 1 and electrical conductivity 1 (arbitrary units). Let an electrical current dipole of unit strength be placed half-way between the center and the top of the sphere. The dipole is directed towards the top of the sphere. Figure 1 depicts a 162-point mesh on the surface of the sphere. The potential generated by the dipole at the points of the mesh can be calculated analytically [12]. In Fig. 2a isopotential lines on the sphere are depicted. This plot has been made by assuming that on each triangle of the mesh the potential varies linearly between the vertices.

We arbitrarily (just for the sake of this demonstration) define 12 "electrode" points on this mesh, as shown in Fig. 1, and take the analytically computed potentials at these points. From the potentials at these points the potentials at the remaining points have been computed by the interpolation methods A and B described above. Figure 2b shows the resulting potential distribution for Method A, and Fig. 2d, the difference with the actual potential distribution. Figures 2c and e are the corresponding results for method B.

The difference between the actual potential distribution and the estimated potential distribution can be expressed by the relative difference: the ratio of the RMS (root mean square) value of the difference between the actual potential distribution **g** and the estimated one **f**, and the RMS value of the actual potential distribution:

$$\text{RELDIF} = \left(\frac{(1/N) \sum_{i=1}^{N} (g_i - f_i)^2}{(1/N) \sum_{i=1}^{N} g_i^2} \right)^{1/2}.$$

The values given below refer to this measure computed over all points in the mesh considered. If the relative difference is zero, the estimated potential distribution is exactly equal to the actual one, and if the relative difference is one, the difference between estimated and actual potential distribution is of about the same size as the potential distribution itself. The relative difference for Method A in this example was found to be 0.413; for Method B it was 0.075. The maximum absolute value of

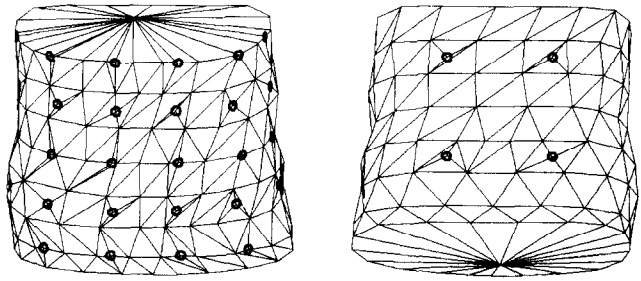

FIG. 3. Triangular mesh of the abdomen of a pregnant woman. The points which are used as "electrode points" are indicated by bold circles. Figure 3a is an anterior view, from slightly above, and Fig. 3b is a posterior view.

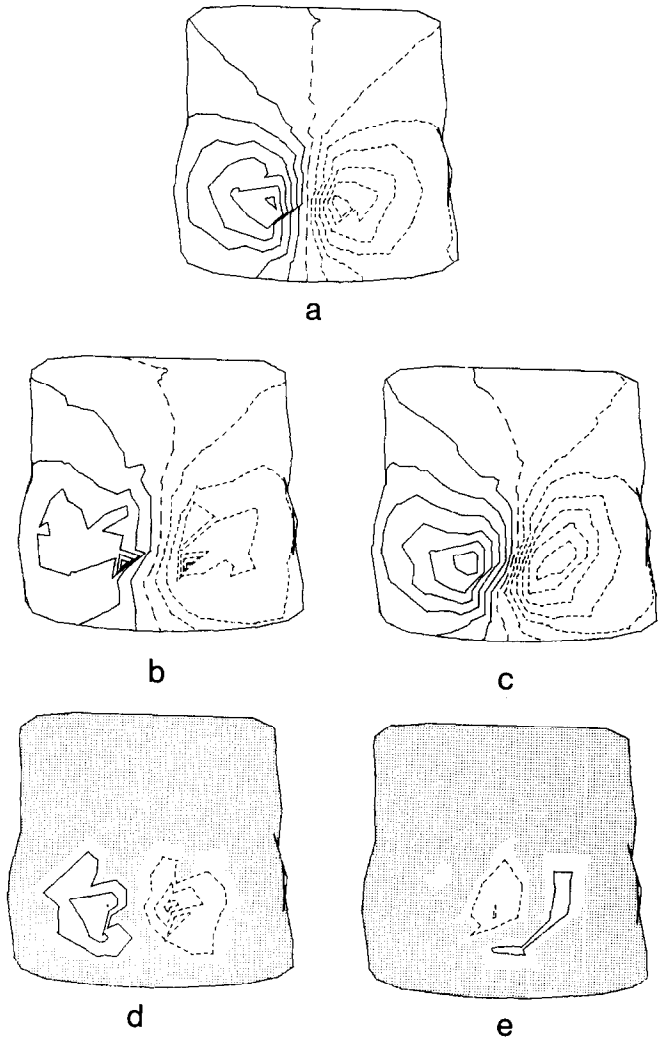

FIG. 4. Plots of isopotential lines on the mesh of Fig. 3 (anterior view). The stepsize between the isopotential lines is the same in all plots. Negative lines are dashed. The zero line is dashed in larger segments. In the difference plots (Figs. 4d and 4e) the area within half a stepsize around zero is shaded: (a) potential distribution on the abdominal surface caused by a current dipole inside the abdomen at the position of the fetal heart as computed by the boundary element method; (b) potential distribution estimated from the potentials at the electrode points (see Fig. 3) as computed by Method *A*; (c) potential distribution estimated from the potentials at the electrode points (see Fig. 3) as computed by Method B; (d) difference between the result of Method A (Fig. 4b) and the actual potential distribution (Fig. 4a); (e) difference between the result of Method B (Fig. 4c) and the actual potential distribution (Fig. 4a).

the potential on the sphere is 0.796. The maximum of the (observed) differences between the actual and the estimated values were 0.242 and 0.050 for Methods A and B, respectively.

(b) Consider the homogeneous volume conductor plotted in Fig. 3. The surface is specified by 192 points. The potential distribution due to a current dipole inside this volume, as found by the boundary element method [2] is shown in Fig. 4.a. This example is taken from a study on the volume conduction aspects of the fetal electrocardiogram [10]. The volume represents the abdomen of a pregnant woman, and the electrical current dipole is located at the position of the fetal heart. Figure 3 also depicts the position of 32 electrodes on this mesh. Figure 4 shows the potential distribution estimated from the potential at the 32 electrodes, using Methods A and B. The relative difference for Method A was found to be 0.266, and for Method B it was 0.156. The maximum absolute value of the potential on the surface is 1.267. The maximum of the differences between the actual and the estimated values were 0.677 and 0.411 for Methods A and B, respectively.

(c) We conclude this section by showing an application of this interpolation method to body surface mapping in cardiography [15, 3]. Figure 5 shows a 398-point mesh of a torso, and the position of 64 surface electrodes. These electrode positions are used in a body surface mapping set-up at the Department of Cardiology of the University Hospital at Nijmegen [6]. Figure 6 shows the potential distribution at all 398 points interpolated by Methods A and B from the data recorded at the 64 electrodes. The potential distribution at 40 ms after onset of the QRS complex is plotted.

V. Discussion

Method A constrains the Laplacian of the function to be zero at the points where the function value is not known. A one-dimensional analogon of this method is a linear interpolation between the points where the function values are known

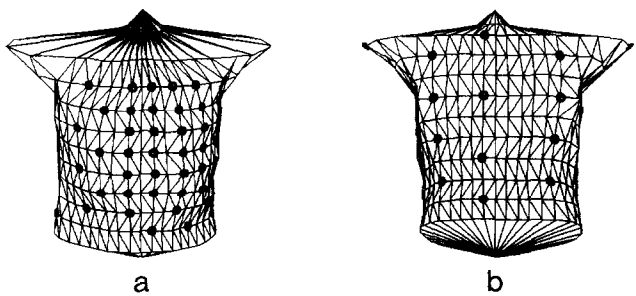

FIG. 5. Triangular mesh of a human torso. The points which are used as "electrode points" are indicated by bold circles. Figure 5a is an anterior view, from slightly above, and Fig. 5b is a posterior view.

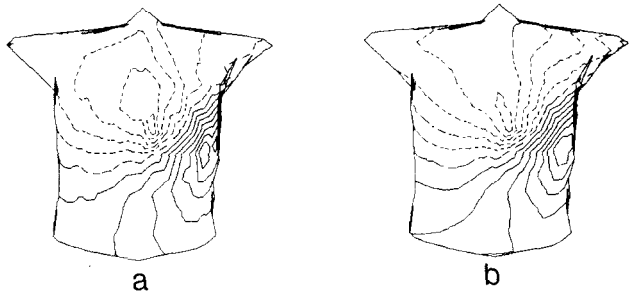

FIG. 6. Plots of isopotential lines on the mesh of Fig. 5 (anterior view). The stepsize between the isopotential lines is the same in all plots. Negative lines are dashed. The zero line is dashed in larger segments: (a) potential distribution estimated from the potentials at the electrode points (see Fig. 5) as computed by Method A; (b) potential distribution estimated from the potentials at the electrode points (see Fig. 5) as computed by Method B.

(Fig. 7a). In a linear interpolation the second derivative (the one-dimensional analogon of the Laplacian) is zero at all points except for those which are being interpolated. In this method, extremes of the function can only occur at points where the function value is known as can be seen by considering the one-dimensional analogon, or by considering the equivalent resistance network model.

Method B minimizes the Laplacian at *all* points. The one-dimensional analogon (Fig. 7b) is similar to a cubic spline. The spline algorithm constructs a continuous function between the points where the function values are known in such a way that the integral of the square of the second derivative is minimized [5, Section 4.4]. This function turns out to be a cubic polynomial. If, in the one-dimensional analogon, the number of points at which the function values are not known approaches infinity the solution approaches the corresponding cubic spline.

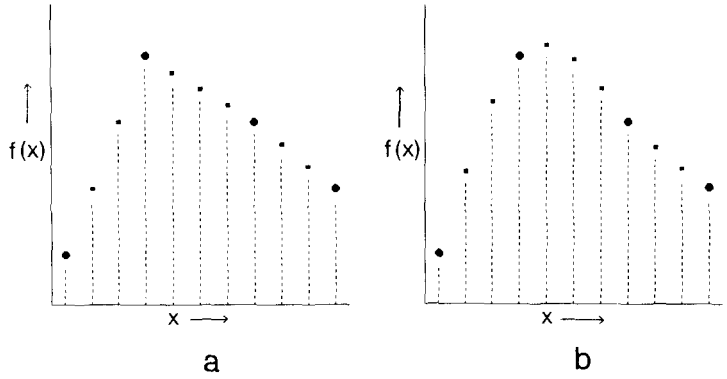

FIG. 7. (a) Plot of the result of the one-dimensional analogon of Method A. The points at which the function values are known are bold. (b) Plot of the result of the one-dimensional analogon of Method B. The points at which the function values are known are bold. They are the same as the ones in Fig. 7a.

In one dimension, Method B yields a smoother line than Method A (Fig. 7). Extremes may occur at positions at which the function values are not known. As a result, Method B may, for instance in potential measurements using electrodes, reconstruct extremes at positions where no electrodes were placed. Method A does not have this ability. This is a manifestation of Earnshaw's theorem [14]. This effect is clearly shown by example b (Fig. 4). Method B finds, reasonably accurately, the position and size of the extremes, in contrast to Method A. Figure 7 indicates that Method B may give better results, as it gives a smoother estimate.

Both examples a and b show that the estimate constructed by Method B resembles the actual functions more closely than does the estimate constructed by Method A. This can be seen by considering the plot of the difference between the estimate and the actual function, as well as by considering the relative difference. In both cases Method B gives a substantially smaller difference. In example c the actual potential distribution is not known. The differences between the results of both methods are substantial at areas where few electrodes are placed.

We have studied the advantage of (the more complex) Eq. (9) as a constraint rather than the simple direct neighbour averaging (Eq. 7) by repeating the computations, now based on Eq. (7). The relative differences in this case were found to be 0.429 and 0.094 in example a for Methods A and B, respectively, and 0.373 and 0.254 in example b, so Eq. (9) gives little improvement over Eq. (7) if the mesh is fairly regular, like in example a, and a large improvement if the mesh is irregular, like in example b. In view of the observed high quality of interpolation procedure B (considering the small number of points at which the function values are considered to be known in the examples), we have refrained from considering more complex approximations to the Laplacian in the most general case [8]. The main purpose of this paper has been to demonstrate that interpolation method A (Laplacian applied to points for which the function values are to be found) may be extended to all points considered (Method B).

The choice to minimize the Laplacian of the function is just one of the many that can be made to construct an interpolation of a function. In general, there is no answer to the question, what interpolation scheme is optimal? The interpolation scheme should be designed according to the general principal that the a priori known properties of the function to be estimated should be incorporated as well as feasible. For instance, if one knows beforehand that the function is linear, one should use an interpolation method which yields linear estimates.

Keeping this general principle in mind, we can see why the minimization of the Laplacian is particularly suited for volume conduction problems. The potential ϕ inside a volume conductor fulfils the equation $\Delta_v \phi = 0$, where Δ_v denotes the Laplacian in three dimensions, at places where there is no current source and the medium is (locally) homogeneous. The value of $\Delta_s \phi$ is, in its discrete form, proportional to the amount of electric current flowing towards the boundary. Since at the boundary the normal component of the electrical current density is essentially zero, the local minimization of $\Delta_s \phi$ is an obvious choice, as is the uniform extension of this constraint over the entire (global) surface. Within this context Method A can

be viewed as treating the volume conductor as a thin (two-dimensional) layer having the shape of the surface of the volume conductor, whereas Method B allows the interior of this surface to become manifest (extension to three dimensions).

In cases where the Laplacian is considered being suitable as a constraint in an interpolation procedure (be it in potential theory or other physical problems in which the Laplacian is zero for the passive part of the medium, like heat conduction, diffusion, etc.) we maintain that this constraint should be applied uniformly to all points considered. That this is indeed possible was demonstrated in this paper.

ACKNOWLEDGMENTS

The authors are grateful for the helpful suggestions of the referees based on an earlier version of this paper, in particular, for pointing out the simple proof of the generalisation of Eq. (7).

REFERENCES

1. M. ABRAMOWITZ AND I. A. STEGUN, *Handbook of Mathematical Functions* (Dover, New York, 1964).
2. R. C. BARR, J. C. PILKINGTON, J. P. BIONEAU, AND M. S. SPACH, *IEEE Trans. Biomed. Eng.* **BME-13**, 80 (1966).
3. R. TH. VAN DAM AND A. VAN OOSTEROM, *Electrocardiographic Body Surface Mapping* (Nijhoff, Dordrecht, 1986).
4. I. S. DUFF AND J. K. REID, *J. Inst. Math. Appl.* **17**, 267 (1976).
5. G. E. FORSYTHE, M. A. MALCOLM, AND C. B. MOLER, *Computer Methods for Mathematical Computations* (Prentice–Hall, Englewood Cliffs, NJ, 1977).
6. A. HERINGA, G. J. H. UIJEN, AND R. TH. VAN DAM, *Electrocardiology '81*, edited by Antaloczy and I. Preda (Akad. Kiado, Budapest, 1982), p. 297.
7. A. HERINGA, G. J. H. UIJEN, R. TH. VAN DAM, AND J. P. J. DE VALK, in *Electrocardiographic Body Surface Mapping*, edited by R. Th. VAN DAM and A. VAN OOSTEROM (Nijhoff, Dordrecht, 1986), p. 171.
8. P. LANCASTER AND K. SALKAUSKAS, *Curve and Surface Fitting* (Academic Press, London, 1986).
9. C. L. LAWSON AND R. J. HANSON, *Solving Least Squares Problems* (Prentice-Hall, Englewood Cliffs, NJ, 1974).
10. T. F. OOSTENDORP, A. VAN OOSTEROM, H. W. JONGSMA, AND P. W. J. VAN DONGEN, *J. Perinat. Med.* **14**, 435 (1986).
11. D. L. PHILLIPS, *J. Assoc. Comput. Mach.* **9**, 84 (1962).
12. R. PLONSEY, *Bioelectrical Phenomina* (McGraw–Hill, New York, 1967).
13. A. ROSENFELD AND A. C. KAK, *Digital Picture Processing*, (Academic Press, New York, 1976).
14. W. R. SMYTHE, *Static and Dynamic Electricity* (McGraw–Hill, New York, 1968).
15. B. TACCARDI, L. DE AMBROGGI, AND C. VIGANOTTI, in *The Theoretical Basis of Electrocardiography*, edited by C. V. Nelson and D. B. Geselowitz (Oxford Univ. Press, Clarendon, Oxford, 1976).